

#### Contents lists available at ScienceDirect

#### **Biomaterials**

journal homepage: www.elsevier.com/locate/biomaterials



## Proteomic analysis of decellularized pancreatic matrix identifies collagen V as a critical regulator for islet organogenesis from human pluripotent stem cells



Huanjing Bi<sup>a</sup>, Kaiming Ye<sup>a,b</sup>, Sha Jin<sup>a,b,\*</sup>

- a Department of Biomedical Engineering, Binghamton University, State University of New York (SUNY), Binghamton, NY, 13902, USA
- b Center of Biomanufacturing for Regenerative Medicine, Binghamton University, State University of New York (SUNY), Binghamton, NY, 13902, USA

#### HIGHLIGHTS

- A proteomic analysis for deciphering cues from decellularized pancreatic materials for islet organoid development.
- Type V collagen induces the formation of human islet organoids that harbor all major pancreatic endocrine cell types.
- Type V collagen augments the generation of endocrine that secrete both glucose level-regulated insulin and glucagon.

#### ARTICLE INFO

# Keywords: Decellularized pancreatic extracellular matrix Proteomics and bioinformatics Matrisome Type V collagen Human induced pluripotent stem cell Islet organoid

#### ABSTRACT

In pancreatic tissue engineering, generating human pancreatic islet organoids from stem cells has been challenging due mainly to a poor understanding of niches required for multicellular tissue self-assembly in vitro. In this study, we aimed to identify bioactive, chemically defined niches from natural, biological materials for islet development in vitro. We investigated the proteomics of decellularized rat pancreatic extracellular matrix (dpECM) hydrogel using advanced bioinformatics analysis, and identified that type V collagen (CoIV) is constantly and abundantly present in dpECM hydrogel. Niches provided to human pluripotent stem cells (iPSCs) by presenting CoIV in matrix coating substrates permitted stem cells progression into islet-like organoids that consist of all major pancreatic endocrine cell types, i.e.  $\alpha$ ,  $\beta$ ,  $\delta$ , and pancreatic polypeptide cells. In the presence of CoIV niches, gene expressions of all key pancreatic transcription factors and major hormone genes significantly increased in iPSC-derived organoids. Most importantly, CoIV-containing microenvironment resulted in enhanced glucose responsive secretions of both insulin and glucagon hormone from organoids. The study demonstrates that CoIV is a critical regulator that augments islet self-assembly from iPSCs, and it is feasible to utilize natural biomaterials to build tissue cues essential for multicellular tissue production in vitro.

#### 1. Introduction

Human pluripotent stem cells (hPSCs), which include pluripotent stem cells (iPSCs), are considered as promising self-renewable primitive cell sources for cell replacement therapy and regenerative medicine [1]. In pancreatic tissue engineering, cadaveric islets are the only resource of human islet organoids, and they are extremely limited resources. Hence, it is important to generate alternatives in the forms of functional hormone-secreting endocrine cells or islets, which will be valuable tissue models for disease modeling, drug screening, and transplantation for diabetes mellitus. However, human islet regeneration in vitro has

had limited success, due in part to poor understanding of tissue niches necessary for islet assembly and development. Although stepwise differentiation approaches have been developed to differentiate hPSCs into insulin-producing cells in vitro [2–6], the generation of intact islets, which comprise of multiple hormone-secreting islet cell types, i.e.  $\alpha$ ,  $\beta$ ,  $\delta$ , and pancreatic polypeptide cells, remains challenging [2]. Results from previous studies suggest that polyhormonal cells may develop into monohormonal cells following transplantation [7–9], indicating that *in vivo* microenvironmental cues are competent for accelerating and enhancing the development of hPSC-derived endocrine cells. Therefore, it is necessary to interrogate cues that mimic the

E-mail address: sjin@binghamton.edu (S. Jin).

<sup>\*</sup> Corresponding author. Department of Biomedical Engineering, Thomas J. Watson School of Engineering and Applied Sciences, SUNY, Binghamton, NY, 13902, USA.

native microenvironment to permit islet self-assembly in vitro.

Tissue extracellular matrix (ECM), a primary microenvironmental component, has been identified as a determinant factor that regulates numerous physiological and pathological processes, such as cell adhesion [10], migration [11], proliferation [12], differentiation [13], inflammation [14], and cancer progression [15] etc. Decellularized pancreatic ECM (dpECM) is a favorable substrate for improving the survival and function of rat islets and mouse  $\beta$ -cells in vitro cultures [16,17]. Narayanan et al. showed that a combination of decellularized ECM and conditioned medium collected from a mouse β-cell line could successfully induce pancreatic differentiation from human embryonic stem cells [18]. Another study conducted by Chaimov et al. demonstrated that dpECM can be used as encapsulation material to support stem cell viability and differentiation into insulin producing cells [19]. Furthermore, a previous study by our group has found that dpECM plays an instructive role in islet organogenesis from hPSCs [20] and that a 3D biomimetic scaffold environment mimicking physiological conditions in the body also permits the formation of islet-like organoids assembled with all four major endocrine cell types [21]. All of these findings imply that natural tissue matrices may serve as unique niches to stem cells for generating functional islet tissues. However, within the tissue matrix, molecules that promote islet organoid development in vitro are largely unidentified.

In this study, we employed proteomics and bioinformatics to identify cues that promote pancreatic islet development from hPSCs. We hypothesized that some dpECM proteins offer instructive cues to direct iPSC islet development. To test this hypothesis, we prepared dpECM from rat pancreas and analyzed its protein profile through proteomics. We discovered that protein contents in the dpECM are remarkably distinct from those in Matrigel. In particular, we identified that type V collagen (ColV) is constantly and abundantly present in the dpECM. Niches provided to cells by blending ColV with Matrigel permitted human iPSCs differentiating into islet organoids that consist of all major pancreatic endocrine cell types, i.e.  $\alpha$ ,  $\beta$ ,  $\delta$ , and pancreatic polypeptide cells. The generated organoids express high levels of pancreatic genes associated with islet identity and function. Most importantly, ColV niches lead to enhanced glucose responsive secretions of both insulin and glucagon from iPSC-derived islet organoids. To the best of our knowledge, these findings, for the first time, unveil the regulatory role of ColV in promoting the generation of human islet organoids in vitro. The study indicates that it is feasible to utilize natural biomaterials to build tissue cues essential for multicellular tissue production in vitro.

#### 2. Materials and Methods

#### 2.1. Preparation of decellularized tissue matrix hydrogel from rat pancreata

Rat pancreata were obtained from the Laboratory of Animal Resources at Binghamton University. Adult male and female Sprague Dawley rats (Charles River) 2-12 weeks old were euthanized by CO2 asphyxiation in accordance with American Veterinary Medical Association (AVMA) guidelines. Pancreata were harvested, pooled, and rinsed with cold PBS twice then stored at -80 °C until use. Before decellularization, the frozen pancreata were cut into 1.5 mm sections using a deli-style slicer (Chef's choice 632, EdgeCraft Corporation) and immediately rinsed with cold deionized water for 5 times at 4 °C with gentle shaking. The entire decellularization process was performed at 4 °C with continuous shaking. The tissue sections were washed with hypertonic solution (10% sodium chloride solution containing 0.1% ammonium hydroxide) for 12 h and deionized water for 12 h. After 4 cycles of hyper/hypotonic washes, the tissue sections were rinsed extensively with deionized water and frozen overnight at -80 °C. The decellularized pancreatic tissues were lyophilized using Freezone freeze dry system (LABCONCO) and grinded using a Wiley Mini Mill (Thomas Scientific). The DNA content of lyophilized, decellularized tissues was quantified using a DNeasy Blood and Tissue Kit (QIAGEN) following manufacturer's instructions. To prepare the tissue matrix hydrogel, 40 mg of lyophilized material powder was solubilized in 2 ml of 0.02 N acetic acid containing 4 mg of pepsin (Sigma- Aldrich, catalogue number P6887) for 48 h at room temperature with continuous stirring, after which the ECM powder was dissolved with very minor or no insoluble fraction. The resultant tissue matrix hydrogel, designated as dpECM, was aliquoted and stored at  $-80\,^{\circ}\text{C}$  until use. Three biological repeats of dpECMs prepared in separate batches from different animals were used in this study.

#### 2.2. Sample preparation for mass spectrometry

Growth factor reduced Matrigel (Corning Life Sciences) and dpECM samples were prepared using a filter-assisted sample preparation method, as described previously [22]. Briefly, samples were dissolved in a lysis buffer containing 5% sodium deoxycholate (SDC), 50 mM Tris-HCl (pH 7.6), and 3 mM dithiothreitol (DTT) at 60 °C. After centrifugation to remove any undissolved particles, the supernatant was transferred to a 30 kD MWCO ultra centrifugal filter (Millipore) and centrifuged at 13,000 g for 30 min. The concentrated sample was exchanged with 1% SDC and 100 mM Tris-HCl (pH 7.6) buffer, then alkylated with 15 mM iodoacetamide in dark for 90 min. Samples were trypsinized with sequencing grade modified trypsin at the enzyme to a sample ratio of 1:100 overnight at 37 °C. Digested peptides were collected and desalted using reversed phase stop-and-go extraction (STAGE) tips as previously described [23]. Peptides were eluted with 80% acetonitrile, 5% ammonium hydroxide and vacuum centrifuged in a SpeedVac (Thermo Fisher) for 1 h to remove volatile components.

#### 2.3. Liquid chromatography-tandem mass spectrometry (LC-MS/MS)

All samples were analyzed on a quadrupole-Orbitrap mass spectrometer (O-Exactive, Thermo Fisher) by Bioproximity Inc. LC was performed on an Easy-nLC 1000 UHPLC system (Thermo) connected with an Easy Spray PepMap column (Thermo, 50 cm x 75 µm I.D.). Mobile phase A (97.5% MilliQ water, 2% acetonitrile, and 0.5% acetic acid) and mobile phase B (99.5% acetonitrile and 0.5% acetic acid) were used to run a LC gradient from 0 to 25% phase B over 210 min, then to 25-80% phase B for 30 min. The mass spectrometer was set to acquire tandem mass spectra from the top 20 ions in the full mass scan at mass range 400–1200 m/z. The dynamic exclusion window was set to 15 s, singly-charged ions were excluded, isolation width was set to 1.6 Da, full MS resolution was set to 70,000 and MS/MS resolution was set to 17,500. The automatic gain control was 2e5 and the normalized collision energy was set to 25, max fill MS was set to 20 ms, max fill MS/MS was set to 60 ms, and the underfill ratio was set to 0.1%. Three biological replicates for Matirgel and three biological replicates using different batches of dpECM hydrogel were analyzed.

#### 2.4. Data analysis

Raw data obtained after LC-MS/MS was converted to MS/MS container files (MGF) format and searched on Amazon Web Services-based cluster compute instances using X!Tandem with the most recent protein sequence libraries available from UniProtKB for the appropriate organism. All searches required 10 ppm precursor mass tolerance, 0.02 Da fragment mass tolerance, strict tryptic cleavage, up to 2 missed cleavages, fixed modification of cysteine alkylation, variable modification of methionine oxidation, and protein-level expectation value scores of 0.0001 or lower. Protein identifications were accepted if they were assigned at least two unique, validated peptides across the analyzed samples with an E-value score of 0.0001 or less. These thresholds resulted in a protein false discovery rate (FDR) of 0.1% [24]. Serum albumin, keratins, and trypsin were considered as contaminants and were excluded from analysis. Relative protein abundance was calculated as a percentage of unweighted spectral count, assigned to each identified

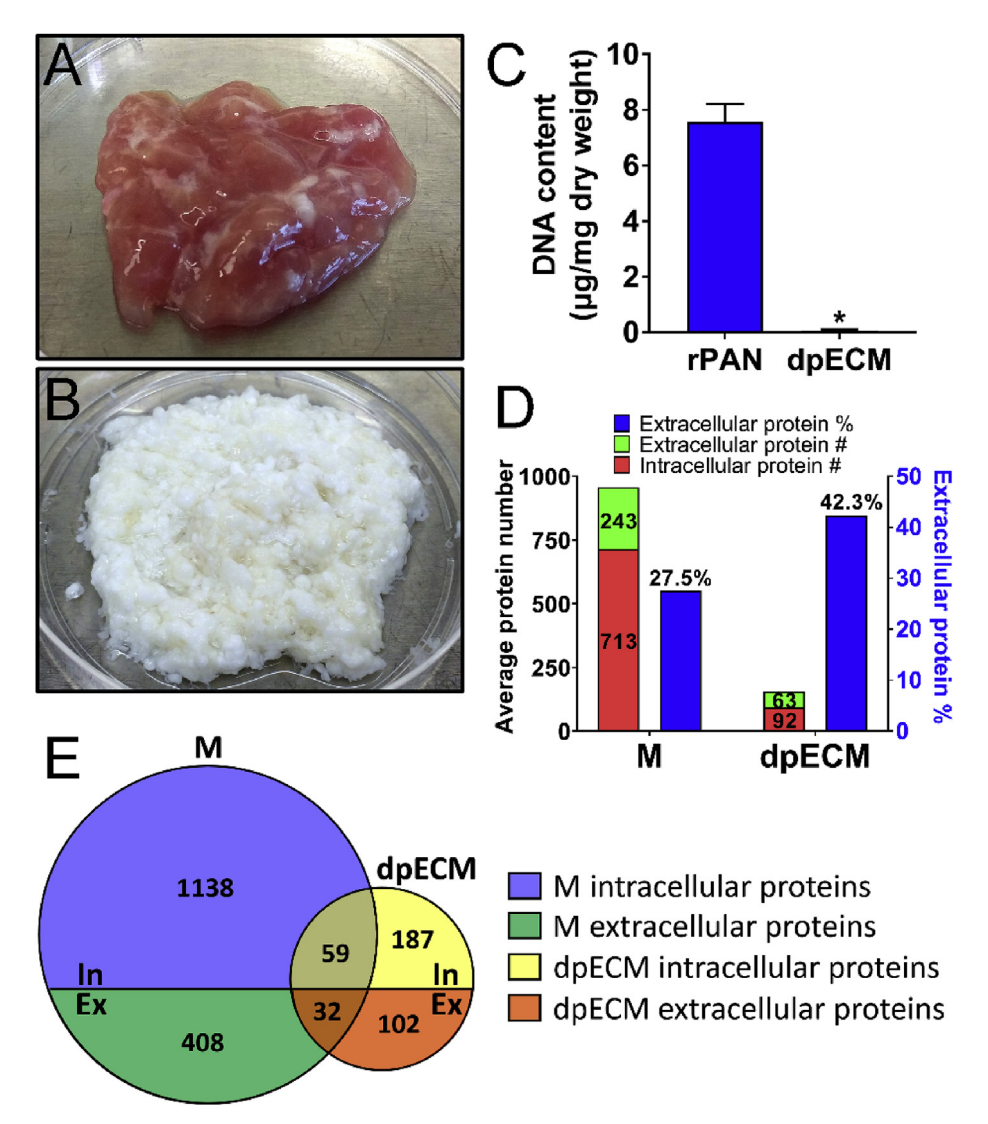


Fig. 1. Characterization and proteomic analysis of decellularized pancreatic ECM. Representative macroscopic images of rat pancreatic tissue before (A) and after (B) decellularization. (C) DNA quantitation of dpECM in comparison to rat pancreatic tissues (rPAN), n = 3. Data are shown as mean  $\pm$  SD. \*, p < 0.05. (D) Average numbers of intracellular and extracellular proteins identified in Matrigel (M) and dpECM, along with the percentage of extracellular proteins in all identified proteins. (E) Venn diagram with total numbers of intracellular (In) and extracellular (Ex) proteins identified in MG and dpECM. n = 3, n = 3, n = 3, n = 3, n = 3.

protein, to the total number of spectra observed in the entire sample. Gene ontology (GO) enrichment analysis was performed using STRAP V1.5.0.0 (Software Tool for Rapid Annotation of Proteins) [25]. Proteins annotated with Gene Ontology terms GO: 0005576 (extracellular region), GO: 0005615 (extracellular space), GO: 0005886 (plasma membrane), and GO: 0009986 (cell surface) were classified as extracellular proteins. Matrisome annotations were identified using MatrisomeDB 2.0 (http://www.matrisomedb.org) [26,27].

#### 2.5. Cell culture and differentiation

Undifferentiated human iPSC line IMR90 was obtained from WiCell Research Institute and routinely cultured on Matrigel-(M, 80  $\mu g/ml)$  coated dishes in mTeSR1 medium (STEMCELL Technologies). Cells were passaged every 4 days at ratios of 1:3 to 1:5. Differentiation was performed as described elsewhere [20]. Briefly, undifferentiated stem cells were harvested using Accutase (STEMCELL Technologies) and seeded onto Matrigel or Matrigel with various amounts of human ColV (Sigma-Aldrich, catalogue number C3657) (M + C)-coated 6-well plates with a density of one million cells/well and cultured in mTeSR1 for 24 h at 37  $^{\circ}$ C in an incubator with 5% CO2. The ColV concentrations

used in this study are: 20 (M + C 20) and 40 (M + C 40)  $\mu g/ml.$ 

The stepwise differentiation protocol used in this study was developed in our lab based on our previous work and those of others [3,4,21,28]. To initiate differentiation, mTeSR1 medium was replaced with differentiation media, as shown in Fig. 5A. Differentiation media in Stage 1 (S1, definitive endoderm) included 50 ng/ml activin A (a TGF-β family member to promote the formation of definitive endoderm, PeproTech) and 1 mM sodium butyrate (NaB, a sonic Hedgehog signaling inhibitor to inhibit liver cell formation, Sigma-Aldrich) in RPMI 1640 (Corning) supplemented with 1 x B27 (Gibco) for 24 h, then the NaB was reduced to 0.5 mM for 3 days. Differentiation media for Stage 2 (S2, posterior foregut) included 250 µM ascorbic acid (Vc, Sigma-Aldrich), 50 ng/ml keratinocyte growth factor (KGF, a FGF family member to promote cell proliferation and differentiation, PeproTech), 50 ng/ml Noggin (a BMP signaling inhibitor, PeproTech), 1 μM retinoic acid (RA, RA signaling for pancreatic development, Sigma-Aldrich), 300 nM (-)-indolactam V (ILV, a protein kinase C activator for pancreatic development, AdipoGen), and 100 nM LDN193189 (LDN, a BMP signaling inhibitor, Sigma-Aldrich) in RPMI 1640 supplemented with 1 x B27 for 5 days. Differentiation media for Stage 3 (S3, pancreatic progenitor) included 1 µM RA, 200 nM LDN, 300 nM ILV, 1 µM 3,3',5-

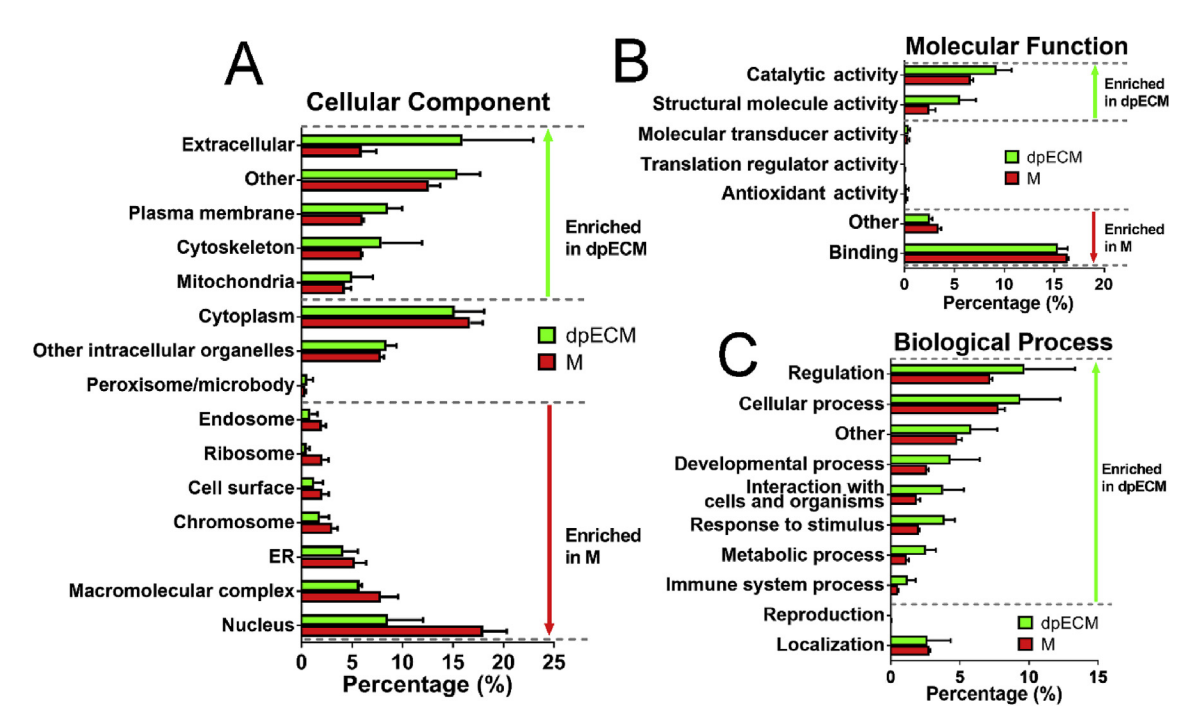


Fig. 2. Enrichment analysis of GO terms for proteins identified in dpECM as compared with those of Matrigel. The proteins were assigned to three main categories: cellular component (A), molecular function (B), and biological process (C). Percentages of these proteins were calculated from protein numbers of individual assignments in the total number of proteins. Data are shown as mean  $\pm$  SD. n (M) = 3, n (dpECM) = 3.

Triiodo- L-thyronine sodium salt (T3, a thyroid hormone to potentiate insulin signaling, Sigma-Aldrich), 10 µM ALK5 inhibitor II (ALKi, a TGF-β signaling inhibitor for pancreatic cell development, Enzo Life Sciences), 10 µg/ml heparin (HP, Sigma-Aldrich) in DME/F12 (Hy-Clone) supplemented with 1 x B27 and glucose to a final concentration of 20 mM for 5 days. Differentiation media in Stage 4 (S4, endocrine lineage) included 1 µM T3, 10 µM ALKi, 1 mM N-acetyl cysteine (N-Cys, a signaling molecule to increase MAFA expression, Sigma-Aldrich), 0.5 µM R428 (a tyrosine kinase receptor AXL inhibitor to induce MAFA expression, SelleckChem), 10  $\mu M$  trolox (a vitamin E derivative for  $\beta$ cell formation, Enzo Life Sciences), 100 nM γ-secretase inhibitor XX (SiXX, a Notch pathway inhibitor for  $\beta$  cell formation, Millipore), 10  $\mu$ M zinc sulfate (Sigma-Aldrich), 10 mM nicotinamide (Nic, a poly (ADPribose) synthetase inhibitor that induces endocrine cell maturation, Sigma-Aldrich), 10 μg/ml HP in RPMI 1640 supplemented with 1 x B27 and glucose to a final concentration of 20 mM for 7 days. Differentiation media in Stage 5 (S5, mature endocrine cells) included CMRL supplement containing either 2% bovine serum albumin (BSA) (Sigma-Aldrich) or 2% fetal bovine serum (Sigma-Aldrich), 1 µM T3, 10 µM ALKi, 0.5 µM R428, 10 mM Nic, and 10 µM H1152 (a ROCK II pathway inhibitor for B cell maturation, Enzo Life Sciences) for 7 days. All differentiation media were changed every two days, unless otherwise specified. For the suspension culture, cells at day 4 of S4 were detached with Dispase (STEMCELL Technologies), dissociated by gentle pipetting, and further cultured in 24-well ultra-low attachment plate with the differentiation media. Half of the medium was changed daily to avoid removing aggregates.

#### 2.6. TaqMan quantitative real-time polymerase chain reaction (qRT-PCR)

Total RNA was extracted at the end of the five-stage stepwise differentiation using an RNeasy Mini Kit (Qiagen), and 200  $\mu$ g of RNA from each sample was analyzed using QuantiTect Multiplex PCR Kit (Qiagen) according to manufacturer's instructions. Primer-probe sets used in this study are listed in Table S1. qRT-PCR was performed using a CFX Connect Real-Time PCR system (Bio-Rad). Non-reversely transcribed RNA and/or no-template samples were used to serve as negative

controls, as described previously in our work [29,30]. Expression values were normalized to cyclophilin as an internal housekeeping gene and then calculated as fold change relative to undifferentiated IMR90 cells cultured on Matrigel using  $\Delta\Delta$ Ct method [[28],]. RNAs extracted from human islets (Prodo Laboratories Inc.) were used as positive controls. For each sample, at least three independent differentiation experiments were performed.

#### 2.7. Immunofluorescence microscopy

At the end of stepwise differentiation, organoids were rinsed with PBS for three times and fixed with 4% PFA for 1 h on ice, followed by an overnight incubation in 30% sucrose solution (w/v) at 4 °C, after which the samples were embedded in optimal cutting temperature compound solution (OCT) (ThermoFisher Scientific) and sectioned at 7 µm thickness. The sections were mounted on TruBond™ Adhesion Slides (Electron Microscopy Sciences) for permeabilization and blocking with Foxp3/Transcription Factor Fixation/Permeabilization (ThermoFisher Scientific) according to manufacturer's instruction. The sections were stained with antibodies as described elsewhere [[20]]. In brief, the sectioned samples were incubated with primary antibodies diluted in blocking buffer overnight at 4 °C and washed with blocking buffer for three times at room temperature. Secondary antibodies were then applied for 1 h at room temperature in the dark, after which the sections were washed, counterstained, and mounted with Vectashield Mounting Medium containing DAPI (Vector Laboratories). Images were captured using a Zeiss 880 multiphoton laser scanning microscope. The images (n = 17-52) of aggregates containing positive endocrine cells (> 3000 cells) under each treatment were quantified to calculate the percentage of each type of endocrine cells in the organoids using the ImageJ software (Version 1.50b, National Institutes of Health). Human islets (Prodo Laboratories Inc.) processed with the same protocol were used as positive controls. All antibodies used in this study are listed in Table S2.

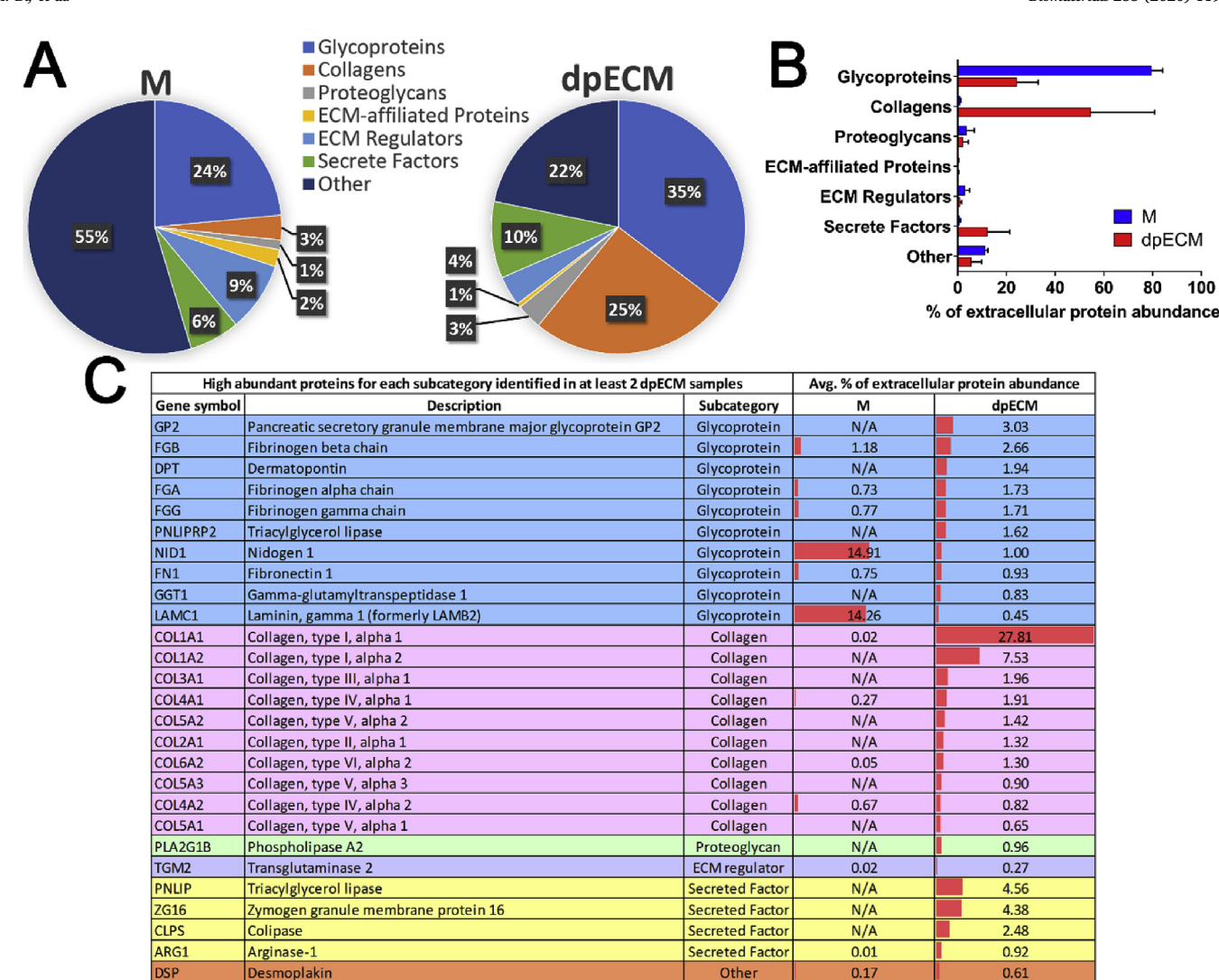


Fig. 3. Matrisome subcategories of extracellular proteins in dpECM and Matrigel. (A) Percentages of proteins under different matrisome subcategories were calculated by dividing the protein numbers of individual matrisome subcategories by the total number of extracellular proteins. (B) Percentage of protein abundance under different matrisome subcategories in the total abundance of extracellular proteins. Data are shown as mean  $\pm$  SD. n (M) = 3, n (dpECM) = 3. (C) A list of high abundant proteins in each matrisome protein subcategory. Proteins identified in at least two batches of dpECM samples were listed, color coded, and sorted by their average percentage of total extracellular protein abundance. The length of red color bars represent the average percentage of each protein in total extracellular proteins, proportional to the percentage. (For interpretation of the references to color in this figure legend, the reader is referred to the Web version of this article.)

#### 2.8. Detection of insulin and glucagon secretion

To measure insulin secretion, serum-free differentiation media were applied for stepwise differentiation. The 2% serum was replaced with 2% BSA in the differentiation medium of Stage 5 to rule out any potential interference from the serum. At the end of differentiation, organoids were washed twice with PBS and preincubated in Krebs-Ringer buffer (KRB) (120 mM sodium chloride, 5 mM potassium chloride, 2 mM calcium chloride, 1 mM magnesium chloride, 5.5 mM HEPES, and 1 mM D-glucose) for 4 h at 37 °C to remove any residual insulin. After rinsing twice with KRB, the cells were separately incubated with KRB containing 2 mM D-glucose, 20 mM D-glucose, or 2 mM D-glucose with 30 mM KCl at 37 °C for 30 min. The respective supernatants were collected and human insulin levels were measured with a human insulin enzyme-link immunosorbent assay (ELISA) kit (ALPCO Diagnostics) according to manufacturer's instructions. Total DNA was extracted from each sample using a DNeasy Blood and Tissue Kit (Qiagen) for normalization. Human islets were used as a positive control.

Voltage-dependent anion-selective channel protein 1

To measure glucagon secretion, the organoids cultured in S5 medium supplemented with 20 mM glucose for 7 days were washed

twice with KRB containing 20 mM glucose and then incubated in the same solution at 37 °C for 4 h. Then the organoids were separately incubated with KRB containing 2 mM D-glucose, 20 mM D-glucose, or 2 mM D-glucose with 30 mM KCl at 37 °C for 30 min. The respective supernatants were collected and human glucagon levels were measured using a human glucagon chemiluminescent ELISA kit (Millipore) according to manufacturer's instructions. Total DNA content from each sample was determined for normalization. Human islets were used as a positive control.

#### 2.9. Statistical analysis

Other

Data are presented as means  $\pm$  standard deviation (SD) of at least three independent experiments. Statistical analysis was calculated by Student's t-test and significance level was set at p values < 0.05.

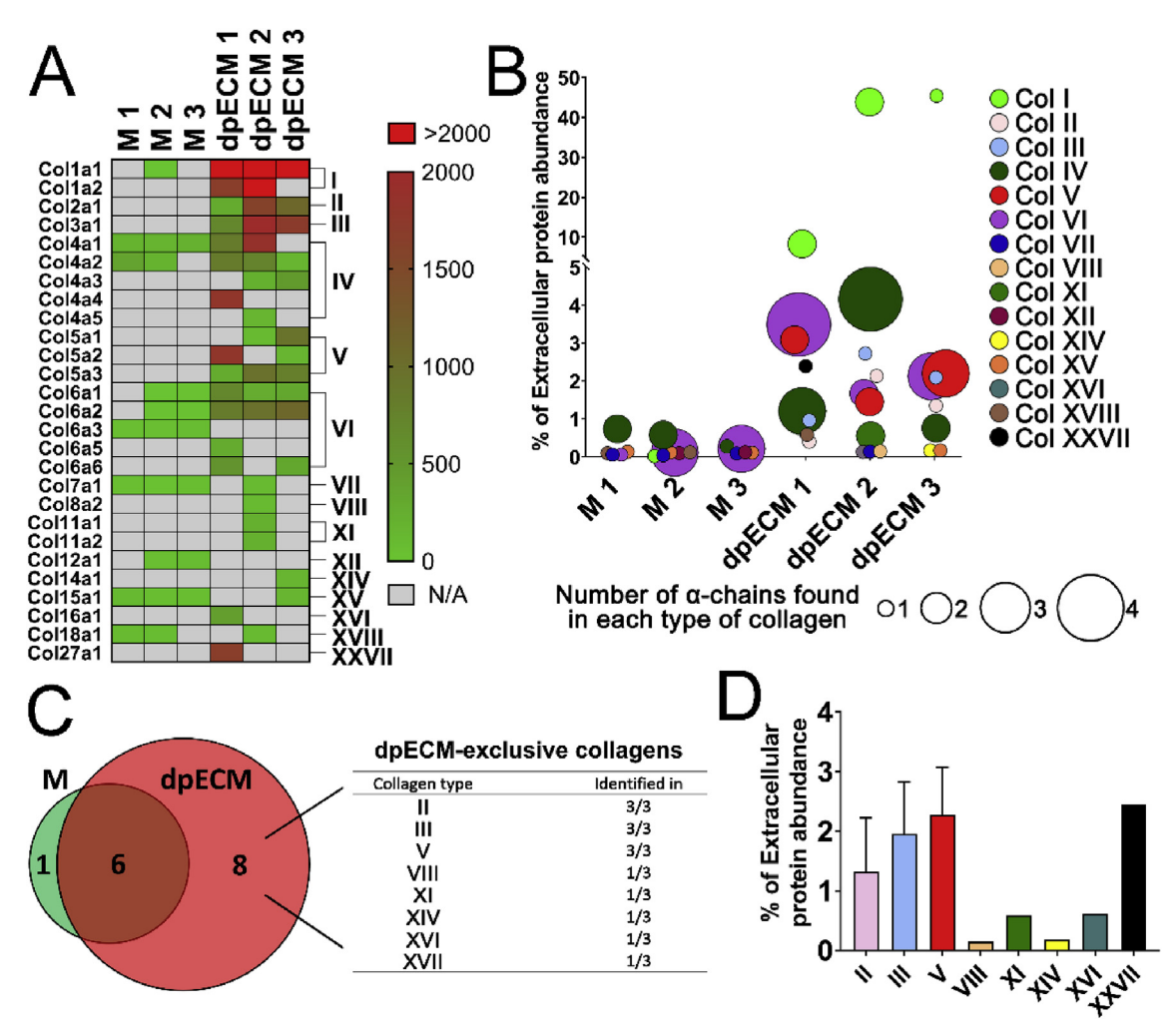


Fig. 4. Comparison of collagen content between dpECM and Matrigel. (A) Heat-map of collagens identified where relative abundance was scaled. Types of collagen, regardless of different types of  $\alpha$  chain, were clustered and shown at the right side of the heat-map. (B) Weighted scatter plot of collagens identified in each sample. Percentages of the relative abundance of each collagen type in total abundance of extracellular proteins were displayed on the Y-axis. Color-code displays different types of collagens and each color indicates one type of collagen. Different sizes of the dots denote the numbers of  $\alpha$  chains identified in each type of collagen. (C) Venn diagram comparing the total number of collagen types identified in dpECM and Matrigel (M). Collagens exclusively identified in three batches of dpECM samples were listed in table. (D) Average percentage of the relative abundance of collagens exclusively identified in dpECM samples in total abundance of extracellular proteins. n = 3, data are shown as mean  $\pm$  SD. (For interpretation of the references to color in this figure legend, the reader is referred to the Web version of this article.)

#### 3. Results

#### 3.1. Proteomic characterization of dpECM materials

The dpECM hydrogel was generated by a detergent-free decellularization method as described in Materials and Methods. After decellularization, the removal of the cellular components was reflected in the color change of pancreatic tissues from cardinal red into clear white (Fig. 1A–B). To evaluate decellularization efficacy, DNA from each batch of dpECM was quantified (Fig. 1C). The residual DNA content in dpECM was only 0.8% of native pancreatic tissue level (61  $\pm$  23 ng/mg in dpECM versus 7567  $\pm$  647 ng/mg in native tissues), which indicates a complete removal of cellular component in the decellularized tissue matrix.

We hypothesized that dpECM hydrogel material contains protein molecules that can function as microenvironmental cues for islet organogenesis. Hence, we characterized the protein composition of dpECM. Growth factor reduced Matrigel, which is commonly used as a supportive substrate for hPSC culture and differentiation, was used for comparison. Throughout mass spectrometry (MS) analysis, we identified an average of 956 proteins from Matrigel samples and 155 proteins

from dpECM samples (Fig. 1D, Table S3). All identified proteins were categorized as either intracellular or extracellular proteins. As expected, Matrigel was dominated by intracellular proteins since Matrigel is a reconstituted extract prepared from basement membrane-rich sarcoma without decellularization (Fig. 1D and E) [32]. On the contrary, dpECM showed a significantly higher proportion of extracellular proteins (42.3%) as compared to Matrigel (25.4%), although the average number of proteins identified in dpECM was limited (Fig. 1D). Collectively, 1637 proteins were identified from three Matrigel samples, including 408 different extracellular proteins (Fig. 1E and Table S4). Among three batches of dpECM samples, 526 proteins were identified, including 134 extracellular proteins (Fig. 1E and Table S4). Matrigel and dpECM only shared 91 proteins in common, out of which 59 were intracellular proteins and 32 were extracellular proteins (Fig. 1E). Taken together, these proteomic results showed distinct protein compositions between Matrigel and dpECM.

#### 3.2. Gene oncology enrichment analysis of the matrix materials

Throughout gene oncology (GO) analysis, we found that the majority of differentially identified proteins enriched in dpECM was

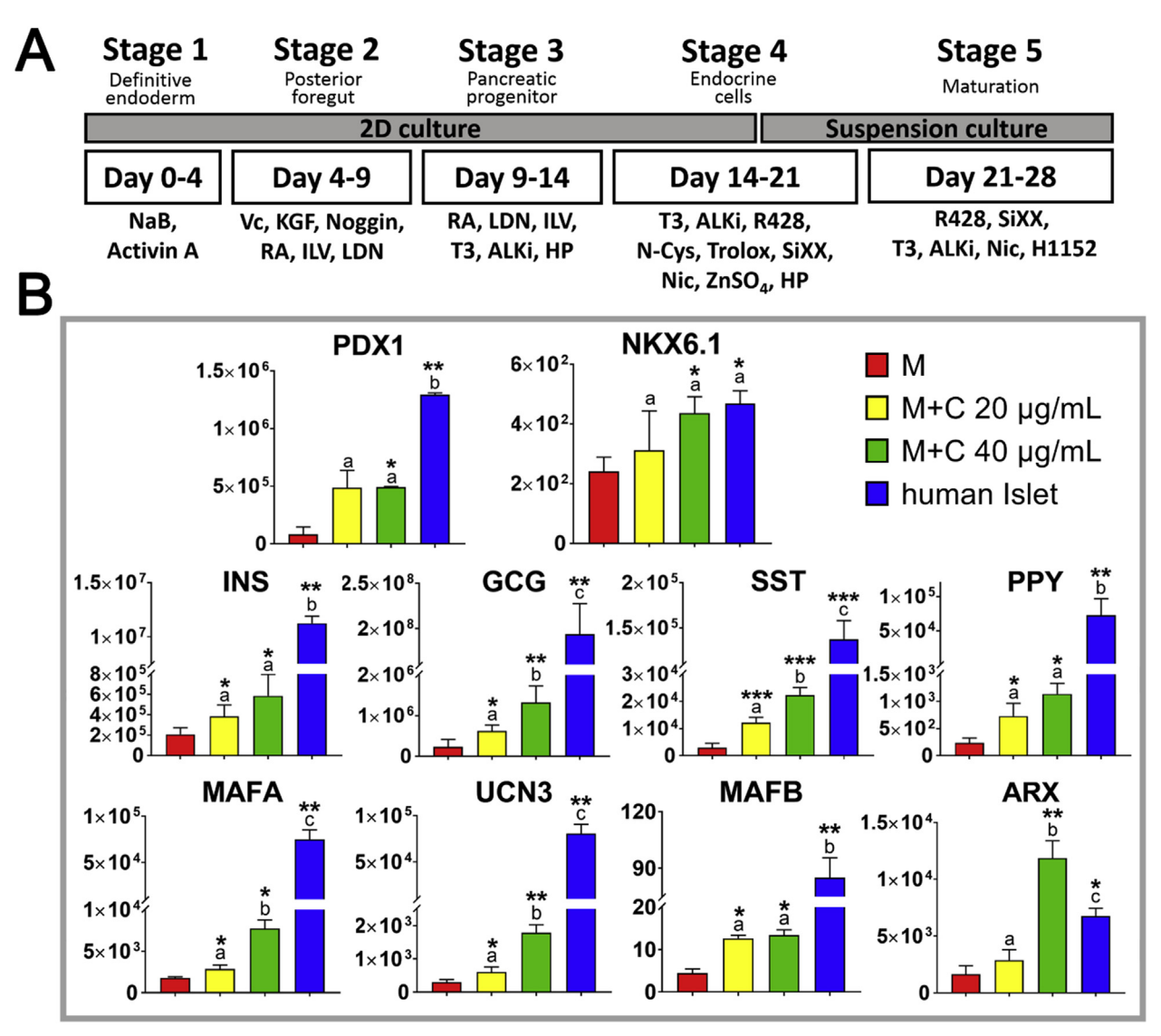


Fig. 5. Enhancement of islet organoid development in the presence of ColV substrates. iPSCs were induced to differentiate to endocrine tissues on Matrigel (M)-coated, or Matrigel and ColV (M + C) mixed substrates-coated plates at indicated ColV concentrations following a five-stage differentiation protocol. (A) Culture method and key signaling molecules used are shown at each stage of differentiation. (B) At the end of five-stage differentiation, organoids were characterized for the expression levels of islet marker genes. The expression levels were normalized to undifferentiated IMR90 cells. Results are from three independent differentiation experiments and shown as mean  $\pm$  SD. \*, p < 0.05; \*\*, p < 0.01; and \*\*\*, p < 0.001 compared to M group. Different letters above the bars represent that the bars are significantly different from each other. Human islet RNA was used as a positive control.

located in the extracellular space and the plasma membrane, while proteins located in cell organelles and the nucleus were highly enriched in Matrigel (Fig. 2A). This is consistent with our finding, noted in Fig. 1D, that Matrigel contained a large quantity of intracellular proteins and showed a smaller extracellular protein proportion than dpECM. In the category of molecular function, a higher percentage of proteins annotated with catalytic activity (GO: 0003824) and structural molecule activity (GO: 0005198) was identified in dpECM samples (Fig. 2B), which indicates that dpECM potentially engages in regulatory activities in pancreatic tissues. A further GO analysis of biological processes showed that proteins associated with biological regulation, cellular process, cell interaction, developmental and metabolic process were significantly enriched in dpECM (Fig. 2C), suggesting that dpECM is closely related to cell behavior and tissue development control. Collectively, the data highlight that, although structurally important proteins for cell binding constitute the bulk of both Matrigel and dpECM, extracellular proteins involved in biological control are higher concentrated in dpECM than in Matrigel.

#### 3.3. Matrisome composition of matrix materials

To better characterize extracellular proteins in dpECM hydrogel, we employed an ECM-specific categorization database, MatrisomeDB 2.0 [33], to analyze the biochemical properties of ECM and ECM-associated proteins (Table S5). Compared with the extracellular proteins in Matrigel, dpECM had larger proportions of glycoproteins, collagens, and a slightly higher proportion of secreted factors in the total number of proteins identified (Fig. 3A). We found consistent results, in that collagens and secreted factors were significantly enriched in dpECM, by comparing the average relative abundances of extracellular proteins in dpECM and Matrigel (Fig. 3B). However, the relative abundance of glycoproteins in Matrigel was higher than that in dpECM, indicating the existence of highly abundant glycoproteins in Matrigel. These observations were validated and illustrated in Fig. 3C, where we listed up to the top 10 abundant proteins attributed to each matrisome subcategory. As expected, we found that major basement membrane glycoproteins such as laminin and nidogen were enriched in Matrigel, while collagens and secreted proteins related to digestive functions of

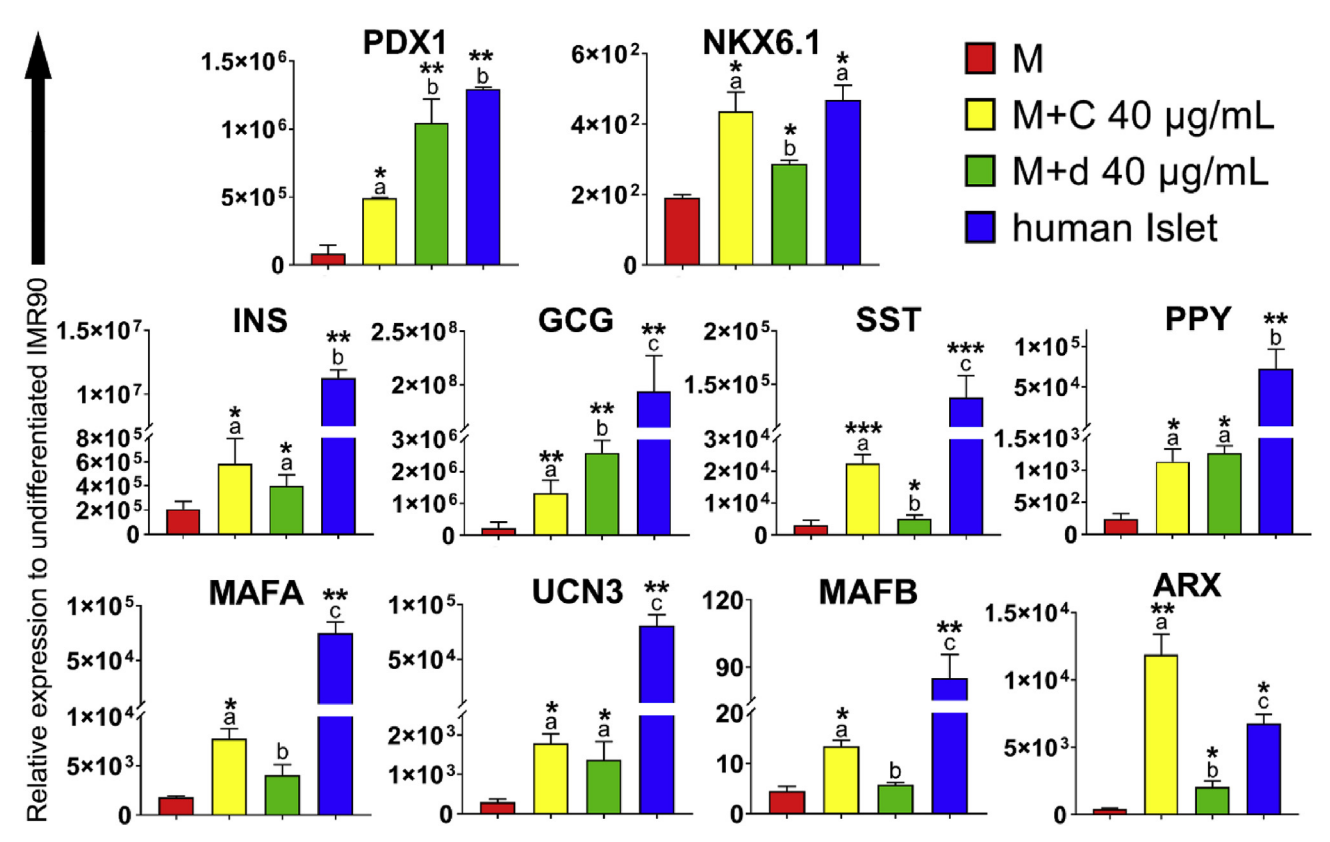


Fig. 6. Comparison of endocrine marker gene expressions in islet organoids developed in the presence of ColV or dpECM substrates. iPSCs were induced to differentiate to endocrine tissues on Matrigel (M)-coated, Matrigel and ColV (M + C) mixed substrates-coated, or Matrigel and dpECM (M + d) mixed substrates-coated plates at indicated concentrations following a five-stage differentiation protocol. At the end of differentiation, the expression levels of endocrine marker genes in the organoids were quantified by qRT-PCR and normalized to undifferentiated IMR90 cells. Results are from three independent differentiation experiments and shown as mean  $\pm$  SD. \*, p < 0.05; \*\*, p < 0.01; and \*\*\*, p < 0.001 compared to M group. Different letters above the bars represent that the groups are significantly different from each other. Human islet RNA was used as a positive control.

the pancreas were proportionally higher in dpECM as compared to that in Matrigel (Fig. 3C).

#### 3.4. ColV exists exclusively in dpECM but not in Matrigel

As noted above, a major difference that we found between the compositions of Matrigel and dpECM was the relatively high abundance of collagens and secreted proteins in dpECM. Since the secreted proteins identified in dpECM were digestive enzymes, which would have minimum effect on stem cell differentiation, we then focused our analysis on the differentially existing collagen contents between Matrigel and dpECM. Our comparative analysis demonstrated that the relative abundance of all the collagen chains identified in dpECM replicates were higher than that in Matrigel samples (Fig. 4A). Likewise, we found that the relative proportions of collagen type II, III, V, and VI in the extracellular proteins of dpECM were significantly higher as compared with those of Matrigel (Fig. 4B). Notably, ColV was the only collagen with all known types of α chain subunits found in dpECM samples in relatively high abundance among the extracellular proteins. Upon comparison of the types of collagen identified in Matrigel and dpECM, we observed that eight types of collagen exclusively exist in dpECM samples, in which type II, III, and V were identified from all three batches of dpECM hydrogel (Fig. 4C). In addition, the proportions of these three types of collagen in extracellular proteins were also relatively high among the proteins found exclusively in dpECM (Fig. 4D). It should be noted that ColV was reported to be present in islets of Langerhans [34] and is indispensable for the proper development and function of  $\beta$ -cells [35]. Furthermore, since only  $\alpha 1$  subunits were identified for other collagens such as Col II and III, given that different α chain subunits may interact with different receptors and trigger

different signaling pathways [34,36], we hypothesized that ColV may play a more important regulative role and can be beneficial or critical for pancreatic islet development from induced differentiation of stem cells. Hence, ColV became the major focus for further investigation in this study.

#### 3.5. ColV promotes islet development from induced differentiation of iPSCs

To validate our hypothesis, we developed five-stage stepwise islet development procedures with a combination of 2D and suspension culture to generate islet-like organoids from iPSCs (Fig. 5A). ColV was used as a coating substrate for seeding cells in tissue culture plates to initiate iPSC differentiation. Since ColV alone as a coating substrate was reported to be antiadhesive toward many cell types [37-39], we blended ColV with Matrigel in a coating solution at the concentrations indicated in Fig. 5B to provide cells with tissue specific cues for endocrine development. At the end of five-stage differentiation, expressions of key endocrine marker genes were detected. Cells that differentiated in the presence of ColV substrate showed significantly higher expression levels of all the endocrine markers examined than those cultured in Matrigel-alone coated plates (Fig. 5B). These markers include key transcription factors PDX1, NKX6.1, MAFA, MAFB, UCN3, and ARX, as well as all the major islet hormone genes insulin, glucagon, somatostatin, and pancreatic polypeptide. Importantly, the increase of ColV concentrations from 20 to 40 µg/ml further, significantly augmented the expressions of glucagon, somatostatin, MAFA, UCN3, and ARX, suggesting that ColV affects endocrine development in a dose-dependent manner (Fig. 5B).

To investigate whether ColV exerts the major regulatory function of dpECM during pancreatic differentiation, we compared the major

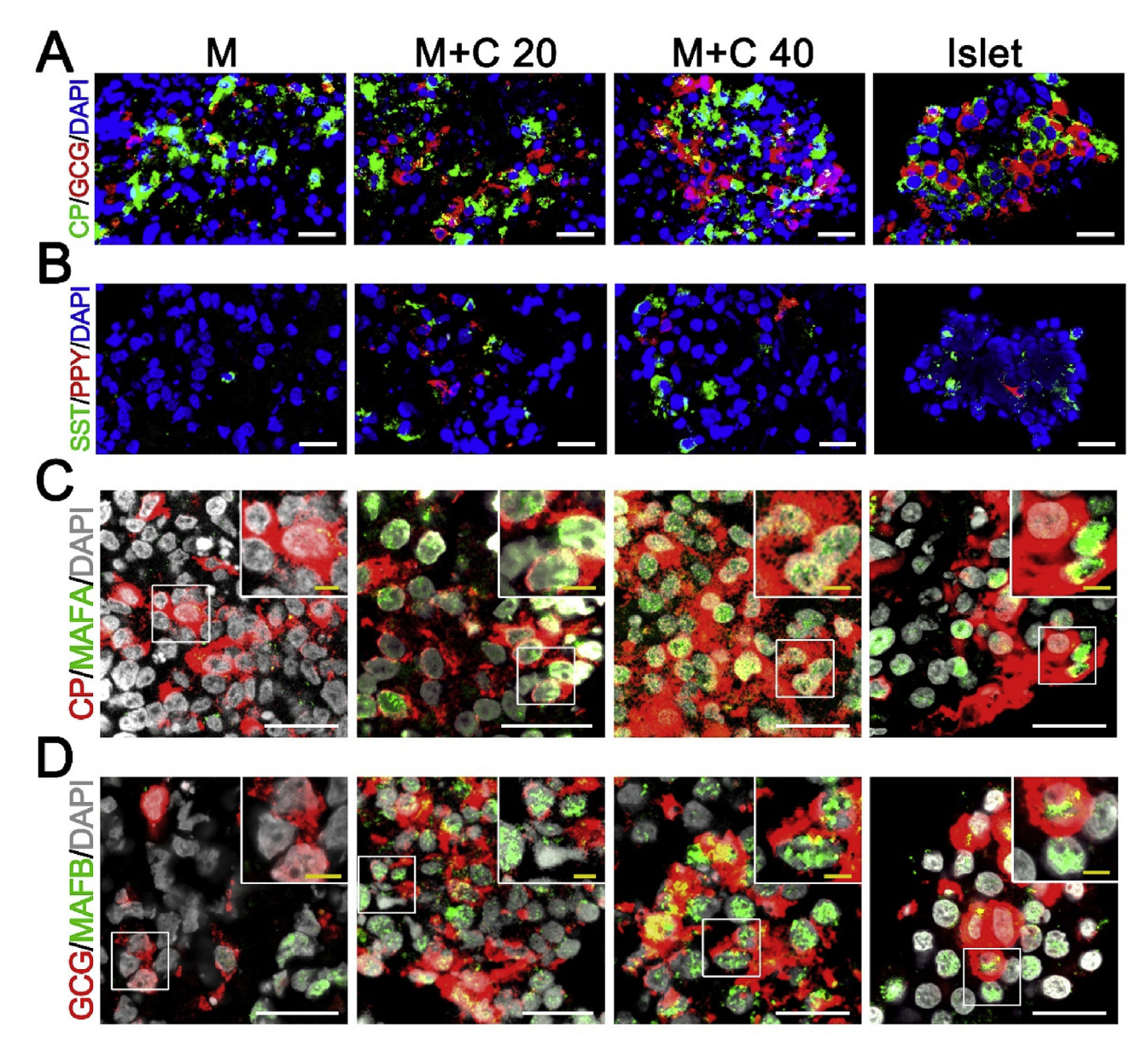


Fig. 7. Enhancement of organogenesis of iPSC-derived islet organoids in the presence of ColV substrates. iPSCs were induced to differentiate to endocrine tissues on Matrigel (M)-coated, or Matrigel and ColV (M + C) mixed substrates-coated plates at the indicated ColV concentrations following a five-stage differentiation protocol. At the end of differentiation, the organoid tissues were immunofluorescently labeled for (A) C-peptide (CP, green) and glucagon (GCG, red); (B) somatostatin (SST, green) and pancreatic polypeptide (PPY, red); (C) MAF bZIP transcription factor A (MAFA, green) and CP (red); and (D) MAF bZIP transcription factor B (MAFB, green) and GCG (red). Cells were counterstained with DAPI (blue). Scale bars, 20 μm. (For interpretation of the references to color in this figure legend, the reader is referred to the Web version of this article.)

endocrine marker gene expressions of Stage 5 aggregates developed on dpECM-containing substrates with those developed on collagen V (ColV)-containing coating substrates (Fig. 6). The experimental results revealed that the expressions of NKX6.1, somatostatin, MAFA, MAFB, and ARX were significantly enhanced in the presence of intensified ColV, as compared to their expressions in dpECM environments. These results were expected, as dpECM only entails very trace amounts of ColV. On the contrary, PDX1 and glucagon gene expressions showed less improvement in ColV cues as compared to dpECM (Fig. 6), suggesting that other components in dpECM might be crucial for inducing the expression of these genes.

To validate the unique role that ColV plays in islet development, we also investigated type I collagen (Col I), another type of collagen identified abundantly in dpECM as shown in Fig. 4A–B. We compared gene expressions of endocrine markers in iPSCs differentiated with M + Col I and M + ColV and found that there were no significant

differences on the gene expression levels of insulin, glucagon, somatostatin, and pancreatic polypeptide between  $M+Col\ I$  and Matrigelalone coating groups, while the  $M+Col\ V$  group showed a significant enhancement (Fig. S1), which indicates type-dependent regulation of collagens in pancreatic differentiation.

3.6. ColV induces the recapitulation of human islet organoids harboring all major pancreatic endocrine cell types from iPSC-derived endocrine cells

To characterize the cellularity and architecture of islet organoids generated, immunofluorescence microscopy was performed to detect all major hormone secreting endocrine cells and their localizations. It should be pointed out that there are no reliable markers that can be used to separate islet organoids from other cell aggregates through flow cytometry. Besides, the efficiency of the generation of islet-like organoids remains low. Therefore, we had difficulty correctly and reliably

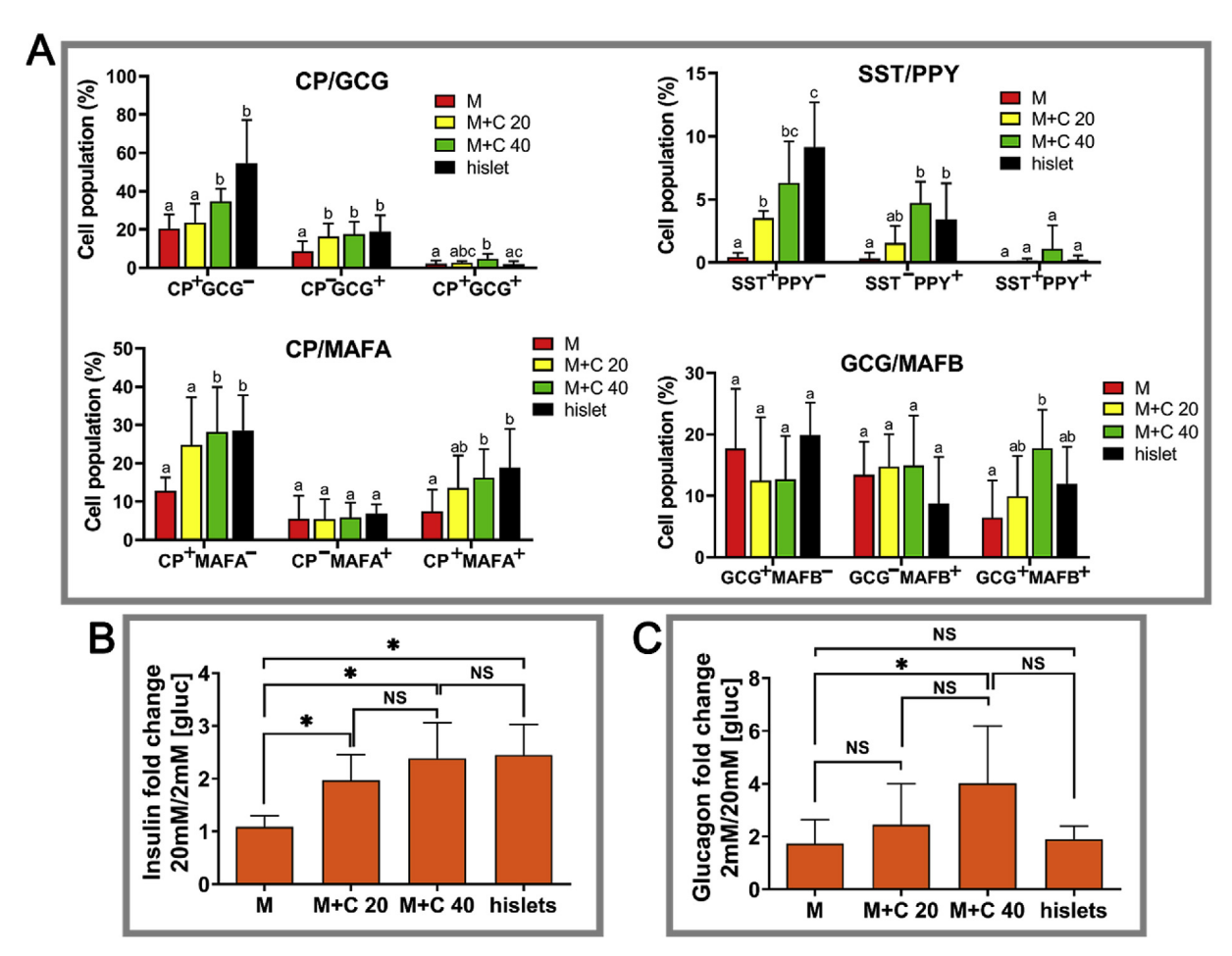


Fig. 8. Characterization of the architecture and glucose-responsive secretions of insulin and glucagon of iPSC-derived islet organoids in the presence of ColV substrates. At the end of differentiation, (A) the organoid structures generated under varied experimental conditions were examined by immunofluorescence staining, followed by semi-quantitative imaging analysis using ImageJ as described in Materials and Methods. Images were quantified to estimate approximate populations of each cell subtype (n = 17-52). Results are shown as mean  $\pm$  SD. Different letters above the bars represent that the groups are significantly different from each other. Human islets (hislet) were used as positive controls. (B) Insulin secretions upon glucose challenge were measured by challenging organoids with low (2 mM) and high (20 mM) concentrations of glucose solution (n = 5 for M group, n = 4 for M + C groups). Fold change was calculated as the ratio of insulin secreted in high glucose conditions to that in low glucose conditions. \*, p < 0.05; (C) Glucose-stimulated glucagon secretion was assessed by challenging organoids with low (2 mM) and high (20 mM) concentrations of glucose solution (n = 5). Fold change was calculated as the ratio of glucagon secreted in low glucose conditions to that in high glucose conditions. Human donor islets (hislet, n = 4) were used as controls. \*, p < 0.05; NS, not significant.

estimating the islet cell subpopulations from the entire population containing many non-islet cells. In order to characterize cell architecture to determine heterogeneity and estimate the organoids' cell composition, we performed cryo-sectioning, immunostaining, and fluorescence microscopy, followed by calculating the percentage of each type of endocrine cells in the organoids using the ImageJ software as reported previously [40]. The images (n = 17-52) of each subtype of islet cells were quantified. We discovered that, in the presence of ColV as a substrate in the early stages of differentiation, iPSC-derived organoids exhibited distributions of insulin-secreting β-cells comparable to that found in human islets (Fig. 7A and Fig. 8A M + C 40 and hislet), where the M + C 40 group yielded 34.7 ± 6.5% c-peptide (CP)-positive cells compare to 54.7  $\,\pm\,\,$  22.5% CP  $^{+}$  cells in human islets. Notably, the percentage of glucagon (GCG)-secreting  $\alpha$ -cells in the M + C 40 group was 17.6  $\pm$  6.5%, which was very close to the population in human islets (18.9  $\pm$  8.6%) (Figs. 7A and 8A). In contrast, cell aggregates formed on Matrigel alone substrates showed significantly less CP<sup>+</sup> and GCG<sup>+</sup> cells (Figs. 7A and 8A M, 20.5 ± 7.4% and 8.8  $\pm$  5.0%, respectively). In addition, both somatostatin-secreting  $\delta$ cells and pancreatic polypeptide-secreting PP-cells were detected in the organoids formed on ColV and Matrigel mixed substrates (Figs. 7B and 8A M + C 20, M + C 40), while no PP-cells were found in the aggregates formed on Matrigel alone substrates (Figs. 7B and 8A). To examine the maturity of these endocrine cells, two critical transcription factors expressed in adult islets, MAFA and MAFB, were dual-stained with CP and GCG, respectively, and imaging analyzed [41,42]. As displayed in Fig. 7C–D and Fig. 8A, elevated proportions of CP $^+/$  MAFA $^+$  and GCG $^+/$ MAFB $^+$  cells were found in the organoids generated in the M + C 40 group, while cells in the aggregates that formed in the Matrigel alone group scarcely expressed these transcription factors (Fig. 8A). These experimental results clearly indicated that ColV plays an important role in recapitulating islet organogenesis during iPSC pancreatic differentiation.

### 3.7. ColV augments glucose-responsive hormone production in iPSC-derived islet organoids

Having characterized the instructive role ColV played in islet organogenesis, we next evaluated the potential of the in vitro generated organoids in controlling glycemic homeostasis under glucose challenge. As shown in Fig. 8B, organoids that differentiated in the presence of the ColV niche showed considerably more glucose-responsive insulin secretion (p < 0.05), while the aggregates cultured on Matrigel alone substrates showed poor responsiveness to sugar level changes. In M + C

40, the insulin fold change in high and low glucose levels is similar to that in human donor islets (Fig. 8B). Another primary glucoregulatory hormone secreted by islets is glucagon, whose secretory response is triggered by hypoglycemia. To evaluate whether the iPSC-derived islet organoids are capable of secreting glucagon in response to glucose levels, we performed glucose-stimulated glucagon secretion (GSGS). We observed that glucose-regulated glucagon secretion from the organoids cultured in the M + C 40 group improved as compared to the control group (p < 0.05) (Fig. 8C). The iPSC-derived organoids showed glucose-regulated glucagon secretion, similar to human islets (Fig. 8C). Taken together, these experimental results revealed that ColV augments the in vitro generation of islet organoids with glucoregulatory secretion of both insulin and glucagon.

#### 4. Discussion

Existing protocols for generating endocrine cells focused on mimicking sequential signaling by using small molecules and growth factors to control differentiation pathways in islet cell development. However, the highly regulated pancreas organogenesis not only relies on proper intracellular signaling, but also requires extracellular niches. The role of an ECM on hPSC differentiation is incomplete, perhaps due partly to its ultra-soft mechanical properties and instable nature. In this study, we have systematically characterized dpECM hydrogel materials to identify unique ECM factors exclusively enriched in the pancreata using advanced proteomics and bioinformatics analyses. Through comprehensive profiling of extracellular proteins in the dpECM material and in vitro islet development approaches, we revealed that ColV acts as an imperative factor that enables the recapitulation and selfassembly of islet organoids from iPSCs. To the best of our knowledge, we discovered, for the first time, that ColV, serving as a substrate coating material, promotes the self-assembly of islet architecture harboring all major pancreatic endocrine cell types. A more important, novel development is that, we were able to acquire both glucose levelregulated insulin and glucagon secretions from iPSC-derived organoids in the presence of ColV stimulation.

ECM is a complex network with tissue-specific composition and a distribution of collagenous and non-collagenous proteins, such as glycoproteins and proteoglycans, which surround cells and influence a variety of biological processes [43]. We used a detergent-free approach to remove all cellular components to maximally preserve the native ECM proteins in the pancreas. Upon decellularization, we reconstituted the dpECM for high resolution MS. To achieve high fidelity (> 99.9%), only proteins with at least 2 unique peptides and < 0.0001 E-value score [24] were analyzed in this study. With these criteria, we obtained a protein list (Table. S4) of 134 extracellular proteins from our dpECM samples (Fig. 1E), more than the previously identified 120 ECM-related proteins in the human pancreas [44], and 11 folds greater than what has been described in the porcine pancreas [45]. The characterization of well-retained dpECM proteins achieved by the combination of our detergent-free decellularization method and high throughput proteomic analysis enabled accurate and sensitive assessment of ECM components including some relatively low abundant proteins that have been unidentified previously.

In addition, our proteomic analysis revealed that the growth-factor-reduced Matrigel contains a significantly lower proportion of ECM proteins compared to dpECM (Fig. 1D). This implies that the preparational procedure of Matrigel, which lacks a decellularization step, leads to the extraction of both structural proteins and large quantities of intracellular proteins. This was confirmed by our GO analysis that numerous cytoplasmic and nuclear proteins were greatly enriched in Matrigel (Fig. 2A). Compared to Matrigel, dpECM was found to be substantially enriched with proteins localized in the extracellular space and on the plasma membrane (Fig. 2A), where most of them were classified as cell-ECM binding proteins such as collagens and junction proteins, and biochemical catalytic enzymes involved in pancreatic

digestion such as triacylglycerol lipase and colipase (Figs. 2B and 3C). Interestingly, dpECM also contains more proteins that regulate cellular process, including but not limited to the control of gene expression, protein modification and interaction, cell communication, proliferation, and differentiation etc. (Fig. 2C) [46]. It should be pointed out that there are a number of proteins unique to each Matrigel or dpECM sample. We speculate that this is due to the presence of numerous lowabundance proteins and the variability of components from different batches of animals, not due to the reproducibility of decellularization and MS characterization, since variations among donor tissues have been reported in a study comparing six patients' tissue matrices [47]. To diminish the variance of low-abundance proteins, we focused data analysis on proteins identified from at least two batches of hydrogel materials prepared from completely different animal donors (Fig. 3C), where a distinct signatures of collagen composition were observed from Matrigel and dpECM materials (Fig. 4). This is consistent with previous studies that collagen is not a major component of Matrigel [48-50], and in sharp contrast to studies where a broad variety of collagen types were identified in ECMs from different tissue/organ sources [49,51,52].

Among the collagens characterized, eight types of collagen were dpECM-exclusive, and type II, III, and V collagens were found in all three batches of dpECM materials in relatively high abundance (Fig. 4C and D). Interestingly, ColV was the only collagen type with all different parent  $\alpha$ -chains identified, i.e.  $\alpha 1(V)$ ,  $\alpha 2(V)$ , and  $\alpha 3(V)$  (Fig. 4A and B). ColV is a relatively minor collagen type in ECM with tissue-specific distribution in the body, including the pancreas [53]. We and the Vigier group [45] identified ColV from rat and porcine pancreatic matrices, which indicates that it is highly conserved in the pancreas across species. In islets of Langerhans,  $\alpha 3(V)$  is a predominant isoform that is preferentially distributed in the pericellular area adjacent to  $\alpha$ - and  $\beta$ cells [54], implying its close relationship to the function of islets. One direct evidence by Huang et al. demonstrated that Col5a3<sup>-/-</sup> mutant mice are glucose-intolerant, insulin-resistant, hyperglycemic, and hypoinsulinemic with decreased islets [35]. In addition, ColVα1 null mutant mice died in utero at approximately embryonic day 10, earlier than the type I and III collagen null mice, suggesting the vital role that ColV plays in the early stages of development [55]. These findings suggest that the in vivo ColV niche is critical for islet development and function, although the role of ColV in vitro tissue/organ development is largely elusive.

During in vitro culture, ColV is reported to be antiadhesive toward many cell types, such as vascular endothelial cells [37], dermal fibroblasts [38], and hepatic stellate cells [39]. We also found that ColV alone as a coating substrate cannot support the attachment of hPSCs (data not shown), while mixing ColV with Matrigel effectively increased hPSC attachment for differentiation. With our five-stage differentiation procedures, we have demonstrated that the expression of key endocrine marker genes were elevated in the presence of ColV (Fig. 5). Of particular interest in islet organogenesis, the cellularity and localization of different types of endocrine cells in organoids generated in the presence of ColV were similar to those of adult islets, indicating that ColV is a unique ECM protein that plays a crucial role in recapitulating islet architecture. Notably, the islet organoids generated by ColV stimulation contained all four types of endocrine cells –  $\alpha$ ,  $\beta$ ,  $\delta$ . and PP cells, which are closely associated with each other (Fig. 7A-B). Such unique heterotypic contacts of endocrine cells in human islets play a central role in regulating β-cell function and maintaining normoglycemia [56]. For example, Rodriguez-Diaz et al. demonstrated that  $\alpha$ cells are capable of releasing paracrine cholinergic signal to the neighboring  $\beta$ -cells, which in turn sensitizes the insulin release of  $\beta$ cells in response to a subsequent increase in glucose concentration [57]. This paracrine interaction is only possible when all the endocrine cells are present in the islet organoid, with a unique cellular arrangement allowing for close association among the cells even after dispersion of the islet [58]. This might be one reason for the enhanced glucose-responsive insulin production from the organoids generated in the

presence of the ColV niche. Upon glucose challenges, no glucose responsive insulin secretion could be detected from the aggregates in the absence of ColV, suggesting a low degree of functionality (Fig. 8B).

In addition, this study demonstrated that organoids generated under ColV niche also secreted glucose-responsive glucagon similar to human islets (Fig. 8C). Our experimental results validated that ColV stimulation facilitates the augmentation of islet organoids' maturity and function. With all the characterizations performed through this work, our experimental data revealed that ColV is a critical regulator that augments in vitro islet development, which benefits the biomaterial society by providing a new understanding of the role of ColV in vitro pancreatic development. Our further investigation will focus on demonstrating the utility of these organoids in islet transplantation for a more direct proof-of-principle of function of the islet organoids.

Taken together, this study discovered ColV as a crucial ECM protein that permits hPSC-derived islet organogenesis, which assembles all major endocrine cells into islet architecture with glucose level-regulated functional hormone secretions. Our experimental results demonstrated that using ColV is a novel strategy for in vitro pancreatic endocrine development and maturation. Knowledge gained from this work will facilitate future developments of clinically relevant islets for disease modeling, drug testing, and transplantation.

#### Declaration of competing interest

The authors declare no competing interests in relation to the work described.

#### Acknowledgements

This work is partially supported by the National Science Foundation CBET1445387, CBET1531944, CBET1928855, and State University of New York Health Now Network of Excellence 68002 (United States). We also thank Kimberly Kal-Downs and Theresa Kolb from Laboratory Animal Resources at Binghamton University for providing rat pancreata and Dr. Tchilabalo Alayi from School of Pharmacy and Pharmaceutical Sciences at Binghamton University for the assistance in mass spectrometry analysis.

#### Appendix A. Supplementary data

Supplementary data to this article can be found online at https://doi.org/10.1016/j.biomaterials.2019.119673.

#### **Author contributions**

HB, SJ, and KY conceived and designed the experiments; HB performed the experiments; HB and SJ analyzed and interpreted the data; HB wrote the manuscript; SJ and KY revised the manuscript. All authors read and approved the final manuscript.

#### Data availability statement

The data generated during the current study are available from the corresponding author on reasonable request.

#### References

- S.M. Wu, K. Hochedlinger, Harnessing the potential of induced pluripotent stem cells for regenerative medicine, Nat. Cell Biol. 13 (5) (2011) 497–505.
- [2] H.A. Russ, A.V. Parent, J.J. Ringler, T.G. Hennings, G.G. Nair, M. Shveygert, T.X. Guo, S. Puri, L. Haataja, V. Cirulli, R. Blelloch, G.L. Szot, P. Arvan, M. Hebrok, Controlled induction of human pancreatic progenitors produces functional beta-like cells in vitro, EMBO J. 34 (13) (2015) 1759–1772.
- [3] A. Rezania, J.E. Bruin, P. Arora, A. Rubin, I. Batushansky, A. Asadi, S. O'Dwyer, N. Quiskamp, M. Mojibian, T. Albrecht, Y.H.C. Yang, J.D. Johnson, T.J. Kieffer, Reversal of diabetes with insulin-producing cells derived in vitro from human pluripotent stem cells, Nat. Biotechnol. 32 (11) (2014) 1121–1133.

[4] F.W. Pagliuca, J.R. Millman, M. Gurtler, M. Segel, A. Van Dervort, J.H. Ryu, Q.P. Peterson, D. Greiner, D.A. Melton, Generation of functional human pancreatic beta cells in vitro, Cell 159 (2) (2014) 428–439.

- [5] B. Rajaei, M. Shamsara, L.M. Amirabad, M. Massumi, M.H. Sanati, Pancreatic endoderm-derived from diabetic patient-specific induced pluripotent stem cell generates glucose-responsive insulin-secreting cells, J. Cell. Physiol. 232 (10) (2017) 2616–2625.
- [6] Z. Ghazizadeh, D.I. Kao, S. Amin, B. Cook, S. Rao, T. Zhou, T. Zhang, Z.Y. Xiang, R. Kenyon, O. Kaymakcalan, C.Y. Liu, T. Evans, S.B. Chen, ROCKII inhibition promotes the maturation of human pancreatic beta-like cells, Nat. Commun. 8 (2017).
- [7] A. Rezania, M.J. Riedel, R.D. Wideman, F. Karanu, Z. Ao, G.L. Warnock, T.J. Kieffer, Production of functional glucagon-secreting alpha-cells from human embryonic stem cells, Diabetes 60 (1) (2011) 239–247.
- [8] A. Rezania, J.E. Bruin, J. Xu, K. Narayan, J.K. Fox, J.J. O'Neil, T.J. Kieffer, Enrichment of human embryonic stem cell-derived NKX6.1-expressing pancreatic progenitor cells accelerates the maturation of insulin-secreting cells in vivo, Stem cells 31 (11) (2013) 2432–2442.
- [9] E. Kroon, L.A. Martinson, K. Kadoya, A.G. Bang, O.G. Kelly, S. Eliazer, H. Young, M. Richardson, N.G. Smart, J. Cunningham, A.D. Agulnick, K.A. D'Amour, M.K. Carpenter, E.E. Baetge, Pancreatic endoderm derived from human embryonic stem cells generates glucose-responsive insulin-secreting cells in vivo, Nat. Biotechnol. 26 (4) (2008) 443–452.
- [10] M. Marsden, D.W. DeSimone, Integrin-ECM interactions regulate cadherin-dependent cell adhesion and are required for convergent extension in Xenopus, Curr. Biol. 13 (14) (2003) 1182–1191.
- [11] K.V. Nguyen-Ngoc, K.J. Cheung, A. Brenot, E.R. Shamir, R.S. Gray, W.C. Hines, P. Yaswen, Z. Werb, A.J. Ewald, ECM microenvironment regulates collective migration and local dissemination in normal and malignant mammary epithelium, P. Natl Acad Sci USA 109 (39) (2012) E2595–E2604.
- [12] E.W. Raines, The extracellular matrix can regulate vascular cell migration, proliferation, and survival: relationships to vascular disease, Int. J. Exp. Pathol. 81 (3) (2000) 173–182.
- [13] H.J. Bi, L.G. Ming, R.P. Cheng, H.L. Luo, Y.J. Zhang, Y. Jin, Liver extracellular matrix promotes BM-MSCs hepatic differentiation and reversal of liver fibrosis through activation of integrin pathway, J. Tissue Eng. Regenerat. Med. 11 (10) (2017) 2685–2698.
- [14] A.S. Chung, W.J. Kao, Fibroblasts regulate monocyte response to ECM-derived matrix: the effects on monocyte adhesion and the production of inflammatory, matrix remodeling, and growth factor proteins, J. Biomed. Mater. Res. A 89 (4) (2009) 841–853.
- [15] P. Lu, V.M. Weaver, Z. Werb, The extracellular matrix: a dynamic niche in cancer progression, The Journal of cell biology 196 (4) (2012) 395–406.
- [16] E. De Carlo, S. Baiguera, M.T. Conconi, S. Vigolo, C. Grandi, S. Lora, C. Martini, P. Maffei, G. Tamagno, R. Vettor, N. Sicolo, P.P. Parnigotto, Pancreatic acellular matrix supports islet survival and function in a synthetic tubular device: in vitro and in vivo studies. Int. J. Mol. Med. 25 (2) (2010) 195–202.
- [17] D. Wu, J. Wan, Y. Huang, Y. Guo, T. Xu, M. Zhu, X. Fan, S. Zhu, C. Ling, X. Li, J. Lu, H. Zhu, P. Zhou, Y. Lu, Z. Wang, 3D culture of MIN-6 cells on decellularized pancreatic scaffold: in vitro and in vivo study, BioMed Res. Int. 2015 (2015) 432645.
- [18] K. Narayanan, V.Y. Lim, J.Y. Shen, W. Tan, D. Rajendran, S.C. Luo, S.J. Gao, A.C.A. Wan, J.Y. Ying, Extracellular matrix-mediated differentiation of human embryonic stem cells: differentiation to insulin-secreting beta cells, Tissue Eng. A 20 (1–2) (2014) 424–433.
- [19] D. Chaimov, L. Baruch, S. Krishtul, I. Meivar-Levy, S. Ferber, M. Machluf, Innovative encapsulation platform based on pancreatic extracellular matrix achieve substantial insulin delivery, J. Control. Release: official journal of the Controlled Release Society 257 (2017) 91–101.
- [20] S. Jin, K. Ye, H. Bi, Microenvironments for self-assembly of islet organoids from stem cell differentiation, US Patent 15 (2017) 841004.
- [21] W. Wang, S. Jin, K. Ye, Development of islet organoids from H9 human embryonic stem cells in biomimetic 3D scaffolds, Stem Cells Dev. 26 (6) (2017) 394–404.
- [22] J.R. Wisniewski, A. Zougman, N. Nagaraj, M. Mann, Universal sample preparation method for proteome analysis, Nat. Methods 6 (5) (2009) 359–362.
- [23] J. Rappsilber, M. Mann, Y. Ishihama, Protocol for micro-purification, enrichment, pre-fractionation and storage of peptides for proteomics using StageTips, Nat. Protoc. 2 (8) (2007) 1896–1906.
- [24] S.T. Rashid, J.D. Humphries, A. Byron, A. Dhar, J.A. Askari, J.N. Selley, D. Knight, R.D. Goldin, M. Thursz, M.J. Humphries, Proteomic analysis of extracellular matrix from the hepatic stellate cell line LX-2 identifies CYR61 and Wnt-5a as novel constituents of fibrotic liver, J. Proteome Res. 11 (8) (2012) 4052–4064.
- [25] V.N. Bhatia, D.H. Perlman, C.E. Costello, M.E. McComb, Software tool for researching annotations of proteins: open-source protein annotation software with data visualization, Anal. Chem. 81 (23) (2009) 9819–9823.
- [26] A. Naba, K.R. Clauser, H. Ding, C.A. Whittaker, S.A. Carr, R.O. Hynes, The extracellular matrix: tools and insights for the "omics" era, Matrix Biol. : journal of the International Society for Matrix Biology 49 (2016) 10–24.
- [27] A. Naba, K.R. Clauser, S. Hoersch, H. Liu, S.A. Carr, R.O. Hynes, The matrisome: in silico definition and in vivo characterization by proteomics of normal and tumor extracellular matrices, Mol. Cell. Proteom.: MCP 11 (4) (2012) M111 014647.
- [28] S. Jin, H. Yao, P. Krisanarungson, A. Haukas, K. Ye, Porous membrane substrates offer better niches to enhance the Wnt signaling and promote human embryonic stem cell growth and differentiation, Tissue Eng. A 18 (13–14) (2012) 1419–1430.
- [29] S. Jin, H. Yao, J.L. Weber, Z.K. Melkoumian, K. Ye, A synthetic, xeno-free peptide surface for expansion and directed differentiation of human induced pluripotent stem cells, PLoS One 7 (11) (2012) e50880.
- [30] N. Hai, D.W. Shin, H. Bi, K. Ye, S. Jin, Mechanistic analysis of physicochemical cues

- in promoting human pluripotent stem cell self-renewal and metabolism, Int. J. Mol. Sci. 19 (11) (2018).
- [32] M.C. Kibbey, Maintenance of the EHS sarcoma and Matrigel preparation, J. Tissue Cult. Methods 16 (3–4) (1994) 227–230.
- [33] O. Clerc, M. Deniaud, S.D. Vallet, A. Naba, A. Rivet, S. Perez, N. Thierry-Mieg, S. Ricard-Blum, MatrixDB: Integration of New Data with a Focus on Glycosaminoglycan Interactions, Nucleic acids research, 2018.
- [34] G. Huang, D.S. Greenspan, ECM roles in the function of metabolic tissues, Trends in endocrinology and metabolism: TEM (Trends Endocrinol. Metab.) 23 (1) (2012)
- [35] G.R. Huang, G.X. Ge, D.Y. Wang, B. Gopalakrishnan, D.H. Butz, R.J. Colman, A. Nagy, D.S. Greenspan, Alpha 3(V) Collagen is critical for glucose homeostasis in mice due to effects in pancreatic islets and peripheral tissues, J. Clin. Investig. 121 (2) (2011) 769–783.
- [36] J. Heino, The collagen receptor integrins have distinct ligand recognition and signaling functions, Matrix Biol.: journal of the International Society for Matrix Biology 19 (4) (2000) 319–323.
- [37] K. Yamamoto, M. Yamamoto, T. Noumura, Disassembly of F-actin filaments in human endothelial cells cultured on type V collagen, Exp. Cell Res. 201 (1) (1992) 55-62
- [38] T. Kihara, Y. Imamura, Y. Takemura, K. Mizuno, E. Adachi, T. Hayashi, Intercellular accumulation of type V collagen fibrils in accordance with cell aggregation, Journal of biochemistry 144 (5) (2008) 625–633.
- [39] K.K. Takai, S. Hattori, S. Irie, Type V collagen distribution in liver is reconstructed in coculture system of hepatocytes and stellate cells; the possible functions of type V collagen in liver under normal and pathological conditions, Cell Struct. Funct. 26 (5) (2001) 289–302.
- [40] R.L. Youngblood, J.P. Sampson, K.R. Lebioda, L.D. Shea, Microporous scaffolds support assembly and differentiation of pancreatic progenitors into beta-cell clusters, Acta Biomater. 96 (2019) 111–122, https://doi.org/10.1016/j.actbio.2019.06. 032.
- [41] T. Matsuoka, I. Artner, E. Henderson, A. Means, M. Sander, R. Stein, The MafA transcription factor appears to be responsible for tissue-specific expression of insulin, P Natl Acad Sci USA 101 (9) (2004) 2930–2933.
- [42] I. Artner, B. Bianchi, J.C. Raum, M. Guo, T. Kaneko, S. Cordes, M. Sieweke, R. Stein, MafB is required for islet beta cell maturation, P Natl Acad Sci USA 104 (10) (2007) 3853–3858.
- [43] M. Riopel, R. Wang, Collagen matrix support of pancreatic islet survival and function. Frontiers in bioscience 19 (2014) 77–90.
- [44] S.D. Sackett, D.M. Tremmel, F. Ma, A.K. Feeney, R.M. Maguire, M.E. Brown, Y. Zhou, X. Li, C. O'Brien, L. Li, W.J. Burlingham, J.S. Odorico, Extracellular matrix scaffold and hydrogel derived from decellularized and delipidized human pancreas, Sci. Rep. 8 (1) (2018) 10452.
- [45] S. Vigier, H. Gagnon, K. Bourgade, K. Klarskov, T. Fulop, P. Vermette, Composition

- and organization of the pancreatic extracellular matrix by combined methods of immunohistochemistry, proteomics and scanning electron microscopy, Current research in translational medicine 65 (1) (2017) 31–39.
- [46] S. Vukicevic, H.K. Kleinman, F.P. Luyten, A.B. Roberts, N.S. Roche, A.H. Reddi, Identification of multiple active growth factors in basement membrane Matrigel suggests caution in interpretation of cellular activity related to extracellular matrix components, Exp. Cell Res. 202 (1) (1992) 1–8.
- [47] T.D. Johnson, R.C. Hill, M. Dzieciatkowska, V. Nigam, A. Behfar, K.L. Christman, K.C. Hansen, Quantification of decellularized human myocardial matrix: a comparison of six patients, Proteom. Clin. Appl. 10 (1) (2016) 75–83.
- [48] C. Hughes, L. Radan, W.Y. Chang, W.L. Stanford, D.H. Betts, L.M. Postovit, G.A. Lajoie, Mass spectrometry-based proteomic analysis of the matrix microenvironment in pluripotent stem cell culture, Mol. Cell. Proteom. 11 (12) (2012) 1924–1936
- [49] K.C. Hansen, L. Kiemele, O. Maller, J. O'Brien, A. Shankar, J. Fornetti, P. Schedin, An in-solution ultrasonication-assisted digestion method for improved extracellular matrix proteome coverage, Mol. Cell. Proteom. 8 (7) (2009) 1648–1657.
- [50] C.S. Hughes, L. Radan, D. Betts, L.M. Postovit, G.A. Lajoie, Proteomic analysis of extracellular matrices used in stem cell culture, Proteomics 11 (20) (2011) 3983–3991.
- [51] Q. Li, B.E. Uygun, S. Geerts, S. Ozer, M. Scalf, S.E. Gilpin, H.C. Ott, M.L. Yarmush, L.M. Smith, N.V. Welham, B.L. Frey, Proteomic analysis of naturally-sourced biological scaffolds, Biomaterials 75 (2016) 37–46.
- [52] O. Rosmark, E. Ahrman, C. Muller, L. Elowsson Rendin, L. Eriksson, A. Malmstrom, O. Hallgren, A.K. Larsson-Callerfelt, G. Westergren-Thorsson, J. Malmstrom, Quantifying extracellular matrix turnover in human lung scaffold cultures, Sci. Rep. 8 (1) (2018) 5409.
- [53] K.M. Mak, C.Y. Png, D.J. Lee, Type V collagen in Health, disease, and fibrosis, Anat. Rec. 299 (5) (2016) 613–629.
- [54] G.R. Huang, D.S. Greenspan, ECM roles in the function of metabolic tissues, Trends Endocrin Met 23 (1) (2012) 16–22.
- [55] R.J. Wenstrup, J.B. Florer, W.G. Cole, M.C. Willing, D.E. Birk, Reduced type I collagen utilization: a pathogenic mechanism in COL5A1 haplo-insufficient Ehlers-Danlos syndrome, J. Cell. Biochem. 92 (1) (2004) 113–124.
- [56] O. Cabrera, D.M. Berman, N.S. Kenyon, C. Ricordi, P.O. Berggrern, A. Caicedo, The unique cytoarchitecture of human pancreatic islets has implications for islet cell function, P Natl Acad Sci USA 103 (7) (2006) 2334–2339.
- [57] R. Rodriguez-Diaz, R. Dando, M.C. Jacques-Silva, A. Fachado, J. Molina, M.H. Abdulreda, C. Ricordi, S.D. Roper, P.O. Berggren, A. Caicedo, Alpha cells secrete acetylcholine as a non-neuronal paracrine signal priming beta cell function in humans, Nat. Med. 17 (7) (2011) 888-U258.
- [58] D. Bosco, M. Armanet, P. Morel, N. Niclauss, A. Sgroi, Y.D. Muller, L. Giovannoni, G. Parnaud, T. Berney, Unique arrangement of alpha- and beta-cells in human islets of Langerhans. Diabetes 59 (5) (2010) 1202–1210.